Molecular Biology of the Cell
Vol. 12, 2672–2687, September 2001

Single Site α-Tubulin Mutation Affects Astral Microtubules and Nuclear Positioning during Anaphase in *Saccharomyces cerevisiae*: Possible Role for Palmitoylation of α-Tubulin

Joan M. Caron,*† Leticia R. Vega,‡ James Fleming,‡ Robert Bishop,§ and Frank Solomon‡

*Department of Physiology, University of Connecticut Health Center, Farmington, Connecticut 06030; ‡Department of Biology and Center for Cancer Research, Massachusetts Institute of Technology, Cambridge, Massachusetts 02139; and §Microbial Expression, Chiron Corporation, Emeryville, California 94608

Submitted September 29, 2000; Revised March 13, 2001; Accepted June 18, 2001
Monitoring Editor: J. Richard McIntosh

We generated a strain of *Saccharomyces cerevisiae* in which the sole source of α-tubulin protein has a cys-to-ser mutation at cys-377, and then we examined microtubule morphology and nuclear positioning through the cell cycle. During G1 of the cell cycle, microtubules in the C377S α-tubulin (C377S *tub1*) mutant were indistinguishable from those in the control (*TUB1*) strain. However, mitotic C377S *tub1* cells displayed astral microtubules that often appeared excessive in number, abnormally long, and/or misoriented compared with *TUB1* cells. Although mitotic spindles were always correctly aligned along the mother-bud axis, translocation of spindles through the bud neck was affected. In late anaphase, spindles were often not laterally centered but instead appeared to rest along the sides of cells. When the doubling time was increased by growing cells at a lower temperature (15°C), we often found abnormally long mitotic spindles. No increase in the number of anucleate or multinucleate C377S mutant cells was found at any temperature, suggesting that, despite the microtubule abnormalities, mitosis proceeded normally. Because cys-377 is a presumptive site of palmitoylation in α-tubulin in *S. cerevisiae*, we next compared in vivo palmitoylation of wild-type and C377S mutant forms of the protein. We detected palmitoylated α-tubulin in *TUB1* cells, but the cys-377 mutation resulted in approximately a 60% decrease in the level of palmitoylated α-tubulin in C377S *tub1* cells. Our results suggest that cys-377 of α-tubulin, and possibly palmitoylation of this amino acid, plays a role in a subset of astral microtubule functions during nuclear migration in M phase of the cell cycle.

INTRODUCTION

Microtubule functions in *Saccharomyce cerevisiae* are apparently simpler than those in higher eukaryotes (reviewed in Solomon, 1991). Previously identified microtubule-dependent functions in this yeast are chromosome separation during mitosis, as well as nuclear migration during mitosis and mating. However, within this relatively limited repertoire, microtubules perform complex functions, forming reversible associations with the cell cortex at precise locations and times during the cell cycle (Goode *et al.*, 1999; reviewed in Heil-Chapdelaine *et al.*, 1999; Miller and Rose, 1999; Adames and Cooper, 2000; Heil-Chapdelaine *et al.*, 2000; Korinek *et al.*, 2000; Lee *et al.*, 2000; Yeh *et al.*, 2000; Farkasovsky and Küntzel, 2001).

† Corresponding author. E-mail address: caron@nso1.uchc.edu.

In *S. cerevisiae*, cytokinesis takes place at the mother-bud neck. Therefore, for equal distribution of chromosomes, the nucleus must first migrate to the bud neck. The mitotic spindle then aligns along the mother-bud axis. This preanaphase nuclear migration and alignment of the spindle require associations between astral microtubules and the cortex of the cell. As the cell enters anaphase, the spindle elongates and is translocated into the bud neck. This second nuclear migration process also requires astral microtubule–cortex interactions.

Several proteins have been identified that assist in both phases of nuclear migration during mitosis. Some proteins (i.e., Kar9p, Bim1p/Yeb1p, Num1p) localize to the tips of the mother and/or bud cortex and capture astral microtubule ends. This microtubule–cortex interaction is thought to move the nucleus to the bud neck. Other nuclear migration proteins (i.e., Dyn1p, Act5p/Arp1p, Nip100p) are required

Table 1. Strains and plasmids

Strain/plasmid	Genotype	Reference
Strains		
FSY279	*a/α; ade2/ADE2; his3Δ200/his3Δ200; leu2-3,112/leu2-3,112; lys2-801/lys2-801; ura3-52/ura3-52* [pWK83; pQX3]	Weinstein and Solomon, 1990
JFY2705	*a/α; ade2/ADE2; his3Δ200/his3Δ200; leu2-3,112/leu2-3,112; lys2-801/lys2-801; ura3-52/ura3-52;* [pWK83; pJFS377]	This study
DBY2384	*α; his3Δ200; leu2-3,112; lys2-801; ura3-52; tub1Δ::HIS3; tub3Δ::TRP1;* [pRB316]	Schatz et al., 1987
LTY430	*α; his3Δ200; leu2-3,112; lys2-801; ura3-52; tub1Δ::HIS3; tub3Δ::TRP1;* [pRB539]	This study
LTY496	*α; his3Δ200; leu2-3,112; lys2-801; ura3-52; tub1Δ::HIS3; tub3Δ::TRP1;* [pLJS214]	This study
LTY429	*α; his3Δ200; leu2-3,112; lys2-801; ura3-52; tub1Δ::HIS3; tub3Δ::TRP1;* [pLJS377]	This study
JBY212	*α; his3Δ200; leu2-3,112; lys2-801; ura3-52; tub1Δ::HIS3; tub3Δ::TRP1;* [pJB2137]	This study
Plasmids		
pWK83	ampR; 2μ; *LEU2-GAL1-10-TUB2*	Weinstein and Solomon, 1990
pQX3	ampR; 2μ; *URA3-GAL1-10-TUB1*	Weinstein and Solomon, 1990
pJFS377	ampR; 2μ; *URA3-GAL1-10-tub1*-C377S	This study
pRB316	ampR; 2μ; *URA3-TUB3*	Schatz *et al.*, 1986
pRB539	ampR; *CEN4-ARS1-LEU2-TUB1*	Schatz *et al.*, 1987
pLJS214	ampR; *CEN4-ARS1-LEU2-tub1*-C214S	This study
pLJS377	ampR; *CEN4-ARS1-LEU2-tub1*-C377S	This study
pJB2137	ampR; *CEN4-ARS1-LEU2-tub1*-C214S/C377S	This study

for spindle movement into the bud neck via sliding of astral microtubules along the surface of the cortex. Both types of astral microtubule–cortex interactions, involving either microtubule tips or microtubule sides, are reversible.

To further investigate microtubule functions during the cell cycle, we constructed a yeast strain such that the sole source of α-tubulin protein was a mutant form in which cys-377 was changed to serine. We chose this residue for site-directed mutagenesis because it corresponds to the primary site of palmitoylation identified in porcine brain α-tubulin (Ozols and Caron, 1997), and it is conserved in all known sequences of α-tubulin. In addition, palmitoylation is a reversible posttranslational modification that is found in membrane-associated proteins but not cytosolic proteins.

We show here that site-directed mutagenesis of cys-377 resulted in astral microtubule defects during anaphase that were strikingly similar to a class of mutations in nuclear migration proteins that are involved in astral microtubule–cortex interactions (i.e., Kar9p, Bim1p/Yeb1p, dynein, dynactin complex proteins). In addition, cys-to-ser mutation of cys-377 reduced in vivo palmitoylation of α-tubulin by >60%. These data suggest that cys-377 of α-tubulin plays a role in astral microtubule-dependent functions during mitosis, perhaps through protein–protein interactions with known nuclear migration proteins, and possibly through lipid–protein interactions via palmitoylated α-tubulin.

MATERIALS AND METHODS

Reagents

Cerulenin (Sigma, St. Louis, MO) was stored at −20°C as a 3 mg/ml stock solution in dimethyl sulfoxide. For labeling, either [9,10-^{3}H]palmitate (specific activity 52 Ci/mmol; PerkinElmer Life Science Products, Boston, MA) or [1-^{14}C]palmitate (specific activity 55 mCi/mmol; PerkinElmer Life Science Products) was dried down in a Savant Speedvac evaporator and redissolved in ethanol to form a 100× stock solution. 4′,6′-Diamidino-2-phenylindole (DAPI; Sigma) was stored at −20°C as a 1-mg/ml stock solution in H_2O. Benomyl (Sigma) was stored at −20°C as a 10-mg/ml solution in dimethyl sulfoxide. A 10× Calcofluor stock (1 mg/ml in H_2O; Sigma) was made immediately before use. Rhodamine-phalloidin (Molecular Probes, Eugene, OR) was stored at −20°C as a 200 U/ml solution in methanol.

Strains and Plasmids

Yeast strains and plasmids are listed in Table 1. We used standard methods for yeast manipulations (Rose *et al.*, 1990; Solomon *et al.*, 1992).

Construction of Haploid tub1 Mutant Strains

The *TUB1:LEU2:CEN4:ARS1*:ampR plasmid pRB539 was mutated with the use of a modification of the Transformer Site Directed Mutagenesis kit (CLONTECH, Palo Alto, CA). Due to the large size of the parental plasmid (~11 kb), we added two primers in addition to the mutation and selection primers, to synthesize the *tub1* plasmids. The two additional primers were AGTCATCGAATTTGATTCTGTGCGATAGCG and AGCGCTTCGTTAATACAGATGTAGGTGTTCC and the selection primer was TGCGGTATTTCACACCGCCCATGGTGCACTCTC. The two additional primers, the selection primer, and the mutagenic primer bound equidistantly around pRB539. Primers used to mutate *TUB1* were designed to change amino acid 377 or 214 from cysteine to serine. To create pLJS377, we used the primer CACAATTGGCTACTGTGGATAGGGCCGTCTCTATGTTGTCAAATACC, which changed codon 377 from TGC (Cys) to AGC (Ser) and introduced a silent mutation that removed an MscI site. To create pLJS214, we used the primer GCTATTTACGACATGAGCAAAAGAAACTTGGACATCCCAAGACC, which changed codon 214 from TGT (Cys) to TCT (Ser) and introduced a silent mutation that removed an *Eco*RV site. Plasmids that lost the appropriate restriction site after mutagenesis were sequenced to confirm that the correct *tub1* mutations were introduced.

To create the double mutant plasmid (pJB2137), pLJS214 was cut with *Hin*dIII. A fragment, containing all of the vector and a majority of the α-tubulin gene, was purified; this fragment was missing the 3′ end of the gene, including the coding region for cys-377. pLJS377 was cut with *Hin*dIII, and the fragment containing the C377S mutation was purified. The C377S fragment was ligated into the C214S fragment. The resulting construct contained a deletion of some of the 3′-noncoding region of *TUB1* in the vector. The plasmid was sequenced to confirm that the correct *tub1* mutations were introduced.

Four plasmids (*TUB1* and the three *tub1* plasmids) were transformed separately into the haploid strain DBY2384 that was deleted for both *TUB1* and *TUB3*, the two α-tubulin genes in *S. cerevisiae*. Before transformation, strain DBY2384 was kept alive by a 2 μ:*TUB3:URA3* plasmid to provide α-tubulin function. Plasmid shuffle (Boeke *et al.*, 1987) was used to replace the *TUB3* plasmid with either *TUB1* or *tub1* plasmids. Transformants were streaked onto 5-fluroorotic acid (5-FOA) plates to select for loss of the *TUB3* plasmid (Boeke *et al.*, 1984). Resulting strains contained as their sole source of α-tubulin either *TUB1* (strain LTY430), C214S *tub1* (strain LTY496), C377S *tub1* (strain LTY429), or C214S/C377S *tub1* (strain JBY212).

Construction of Diploid C377S tub1 Overexpressor Strain

To construct the C377S *tub1* overexpressor plasmid (pJFS377), pQX3, which contains *GAL1–10-TUB1*, was cut with *Bst*EII and BsrGI. A fragment, containing all of the vector and a majority of the *TUB1* gene, was purified. This fragment was missing the 3′ end of the *TUB1* gene, including the coding region for cys-377. pLJS377 was cut with *Bst*EII and BsrGI, and the fragment containing the C377S *tub1* mutation was purified. The C377S *tub1* fragment was ligated into the *GAL1–10-TUB1* fragment. The resulting construct was sequenced to confirm that the correct *tub1* mutation was introduced.

The diploid strain FSY279 was streaked onto 5-FOA plates to select for loss of the *GAL1–10-TUB1* plasmid (pQX3). Cells were then transformed with three different *GAL1–10*-C377S *tub1* plasmids. Transformed strains were maintained in synthetic complete (SC) medium (−U, −L). To assess galactose induction of Tub1p and C377S tub1p synthesis, strain FSY279 (containing the *GAL1–10-TUB1* plasmid) and strains containing the *GAL1–10*-C377S *tub1* plasmids were grown for up to 4 h in SC (−U, −L) and 2% galactose. At several time points, cells were lysed and extracts were assayed for relative levels of α- and β-tubulin by SDS-PAGE and immunoblot analysis. Strain JFY2705 produced similar levels of α-tubulin as strain FSY279 at all time points. After 4 h in the presence of galactose, α-tubulin levels increased by approximately fivefold and β-tubulin increased by approximately twofold in both strains.

Microscopy

Microtubules were visualized with the use of the rat monoclonal anti-tubulin antibody YOL1/34 and fluorescein isothiocyanate-labeled goat anti-rat antibody (Rose *et al.*, 1990; Solomon *et al.*, 1992). Nuclei were visualized by staining with DAPI. Bud scars were visualized by staining with Calcofluor (Rose *et al.*, 1990). Actin filaments and cortical actin patches were visualized by staining with rhodamine-phalloidin (Miller *et al.*, 1999). Cells were viewed at the Center for Biomedical Imaging Technology, University of Connecticut Health Center, Farmington, CT, with a Zeiss Axiovert 100 microscope equipped with a 63×/1.25 or 63×/1.40 objective lens. Images were recorded with a cooled charged-coupled device camera (Photometrics, Phoenix, AZ). Differential interference and phase contrast microscopy was performed with the same system.

Immunoblot Analysis

Immunoblot analysis of α- and β-tubulin levels was performed with rabbit polyclonal anti-α-tubulin (#345) and anti-β-tubulin (#206) antibodies (Weinstein and Solomon, 1990), with the use of enhanced chemiluminescence detection (Amersham Pharmacia Biotech, Arlington Heights, IL).

Benomyl Sensitivity

To examine benomyl sensitivity, serial dilutions of cells were placed onto YPD plates containing benomyl (0–40 μg/ml) at 10 μg/ml increments. Plates were incubated at various temperatures until control plates, containing no benomyl, showed confluent growth.

In Vivo Palmitoylation of Yeast Proteins and Immunoprecipitation of Tubulin

Strains FSY279 and JFY2705 were grown overnight at 30°C in SC medium containing 2% raffinose. At the zero time point, cells (2×10^8) were inoculated into 1 ml of YP medium containing 2% galactose. The pH of the media was adjusted to 6.8; this has been found to increase uptake of exogenous palmitate (Powers *et al.*, 1986). To reduce endogenous levels of palmitate, cerulenin was added to a final concentration of 3 μg/ml (Funabashi *et al.*, 1989). Incubation of FSY279 cells with cerulenin for 4 h did not affect the percentage of large-budded cells, nor did it alter the extent or pattern of microtubules (Caron, unpublished data). After 3 h at 30°C, [^{3}H]palmitate (1 mCi/ml) was added. In one set of experiments, [^{14}C]palmitate (0.1 mCi/ml) replaced [^{3}H]palmitate because carbon 14 is a stronger beta-emitter than tritium. Cells were incubated for an additional hour and then washed once in ice-cold lysis buffer (phosphate-buffered saline, 1% Triton X-100, 0.5% SDS, 1 mM β-mercaptoethanol). Cell pellets were frozen in dry ice/ethanol, and resuspended in 300 μl of lysis buffer containing protease inhibitors (Caron, 1997). An equal volume of glass beads was added, and cells were broken by vortexing six times in 1-min bursts followed by chilling on ice. Insoluble material was removed by centrifugation at 14,000 × *g* for 10 min at 4°C. Protein concentrations of resulting supernatants were determined with the DC Protein Assay kit (Bio-Rad, Richmond, CA).

To examine [^{3}H] or [^{14}C]palmitoylated proteins in whole cell extracts, yeast proteins were precipitated with chloroform/methanol (Wessel and Flügge, 1984), resuspended in sample buffer (Laemmli, 1970), and analyzed by one-dimensional (1D)-PAGE and fluorography.

To immunoprecipitate either α- or β-tubulin, cell lysates (1 mg) were diluted fivefold with immunoprecipitation buffer (phosphate-buffered saline, 1% Triton X-100, 1 mM EGTA, and protease inhibitors) and incubated with an excess of the mouse monoclonal antibody A1BG7 for α-tubulin or B1BE2 for β-tubulin (Vega *et al.*, 1998). Under these lysis and immunoprecipitation conditions, α- and β-tubulin did not coimmunoprecipitate (Caron *et al.*, 1985; Caron, unpublished data). Immunoprecipitated proteins were subjected to 1D-PAGE (Laemmli, 1970) with the use of dithiothreitol (10 mM) as the reducing agent. Gels were stained with Coomassie blue, photographed with an α-Innotech IS-1000 Digital Imaging System, and fluorographed with Kodak X-OMAT AR x-ray film at −70°C. Approximately 10% of the immunoprecipitated protein was subjected to immunoblot analysis to determine α- and β-tubulin levels.

In Vivo Palmitoylation of Yeast Proteins and DEAE Chromatography of Tubulin

Strains FSY279 and JFY2705 were grown overnight at 30°C in SC medium containing 2% raffinose. At the zero time point, cells (2×10^8) were inoculated into 20 ml of YP medium (pH 6.8) containing 2% galactose. Cerulenin was added to a final concentration of 3 μg/ml. After 4 h at 30°C, [^{3}H]palmitate (0.1 mCi/ml) was added.

Cells were incubated for an additional hour and then washed twice with ice-cold distilled water, frozen in dry ice/ethanol, and resuspended in 300 μl of lysis buffer (0.1 M piperazine-*N*,*N*′-bis(2-ethanesulfonic acid) [PIPES], pH 6.8, 10 mM $MgSO_4$, 2 mM EGTA, 0.1 mM GTP, 5 mM dithiothreitol, 1% Triton X-100) with protease inhibitors (1 μg/ml antipain, 1 μg/ml aprotinin, 2 μg/ml leupeptin, 2 μg/ml pepstatin A, 2 μg/ml chymostatin, 1 mM N-α-*p*-tosyl-L-arginine methyl ester). An equal volume of glass beads was added, and cells were broken by vortexing six times in 1-min bursts followed by chilling on ice. Supernatants were transferred to fresh tubes. Beads were washed with 200 μl of lysis buffer, and the second set of supernatants was combined with the first. Additional protease inhibitors (2 mM phenylmethylsulfonyl fluoride, 1 mM benzamidine, 5 mM phenanthroline) were added. Supernatants were centrifuged first at 1,086 × *g* for 10 min followed by 100,000 × *g* for 60 min at 4°C.

DEAE chromatography was performed as described by Barnes *et al.* (1992) with some modifications. All procedures were performed at 4°C. Glycerol and NaCl were added to supernatants to final concentrations of 10% and 0.1 M, respectively. Supernatants (~2.2 mg of protein per strain) were loaded onto 1-ml columns of DE-52 resin (Whatman, Clifton, NJ) equilibrated with column buffer (0.1 M PIPES, pH 6.8, 10 mM $MgSO_4$, 2 mM EGTA, 0.1 mM GTP, 0.1 M NaCl, 10% glycerol, 1% Triton X-100, and protease inhibitors). The column was washed with 5 volumes of column buffer. Tubulin was eluted with 2 volumes of bump buffer (0.1 M PIPES, pH 6.8, 10 $MgSO_4$, 2 mM EGTA, 0.1 mM GTP, 0.6 M NaCl, 10% glycerol, 1% Triton X-100, and protease inhibitors). Fractions (100 μl) were collected.

Duplicate samples of each fraction were subjected to SDS-PAGE followed by either Coomassie blue staining or immunoblot analysis of α-tubulin levels. Fractions containing tubulin were pooled and proteins were concentrated by chloroform/methanol precipitation (Wessel and Flügge, 1984). Precipitated protein was solubilized in sample buffer (Laemmli, 1970), and duplicate samples were subjected to SDS-PAGE followed by either Coomassie blue staining and fluorography or immunoblot analysis of α-tubulin levels.

RESULTS

Generation of TUB1, C377S tub1, C214S tub1, and C214S/C377S tub1 Haploid Strains

We used site-directed mutagenesis to construct plasmids in which either cys-377 or cys-214 or both of *TUB1* was changed to serine. The haploid yeast strain DBY2384 was transformed with either the *TUB1*, C377S *tub1*, C214S *tub1*, or C214S/C377S *tub1* plasmids. Strain DBY2384 has deleted copies of chromosomal *TUB1* and *TUB3*, the two α-tubulin genes in *S. cerevisiae*, but contains a plasmid with *TUB3* for α-tubulin function, and *URA3* as a selective marker. Transformants were obtained for all four plasmids indicating that coexpression of C377S *tub1*, C214S *tub1*, or C214S/C377S *tub1* with *TUB3* was not deleterious to the cells. When transformants were grown on 5-FOA to select for the ability to lose the *TUB3* plasmid (Boeke *et al.*, 1984), colonies were obtained with either *TUB1*, C377S *tub1*, C214S *tub1*, or C214S/C377S *tub1* as their sole source of α-tubulin. These results demonstrate that neither cys-377 nor cys-214 is essential.

Morphology of TUB1 and tub1 Mutant Haploid Strains

We examined whether the cys-to-ser α-tubulin mutations affected microtubules or position of nuclei in cells grown at 30°C. Cells were processed for immunofluorescence microscopy of microtubules and DAPI staining of DNA as described in MATERIALS AND METHODS. In G1 of the cell cycle, *TUB1* cells contained a set of short astral microtubules emanating from a single site on the nuclear membrane into the cytoplasm. All three *tub1* mutants displayed the *TUB1* microtubule configuration while in G1 (Figure 1A).

As cells entered mitosis, spindles in all four strains oriented along the mother-bud axis. In anaphase, astral microtubules in *TUB1* cells emanated from both ends of the spindle until reaching the cortex of both the mother and bud. As spindles continued to elongate, astral microtubules shortened and chromosomes moved to the cortex of both the mother and bud.

In contrast to *TUB1* cells, abnormal microtubule phenotypes were pronounced in mitotic cells expressing C377S tub1p: ~45% of mitotic C377S *tub1* cells displayed at least one of the abnormal astral microtubule structures shown in Figure 1, C–H. These cells often appeared to contain an excess number of astral microtubules, some of which were abnormally long and were bent around the periphery of the cell (Figure 1, C–H). Some astral microtubules in the C377S *tub1* mutant were also incorrectly oriented: as shown in Figure 1, E and F, astral microtubules emerging from the spindle pole body nearest the bud grew into the mother cell instead of the bud. Abnormally long mitotic spindles (Figure 1C) were also observed in the C377S *tub1* cells.

The majority of mitotic C214S *tub1* cells were indistinguishable from *TUB1* cells (Figure 1B and accompanying table). However, a small number of mitotic C214S *tub1* cells (12%) displayed long astral microtubules that curved around the cortex of the bud. Abnormally long spindles were not found in either *TUB1* or C214S *tub1* cells.

The double mutant C214S/C377S *tub1* was indistinguishable from the C377S *tub1* mutant, displaying similar patterns of aberrant astral microtubule arrays and abnormally long spindles during anaphase. However, the abnormal microtubule phenotype of the double mutant appeared no more pronounced than that of the single mutant C377S *tub1*: ~39% of the C214S/C377S *tub1* cells had abnormal astral microtubules, 6% had long spindles, and 55% resembled *TUB1* cells.

When cells were grown at 15°C, microtubules in *TUB1*, C377S *tub1*, and C214S *tub1* cells were again indistinguishable during G1 of the cell cycle. During mitosis, microtubule patterns in C214S *tub1* cells were most often (94%) indistinguishable from those in *TUB1* cells (Figure 2A). In contrast, ~31% of mitotic C377S *tub1* cells displayed abnormally long mitotic spindles that bent around the periphery of the mother or the bud or both. In some cases, elongated spindles formed a "figure 8" pattern (Figure 2B), whereas other spindles were shaped like a question mark with the longer, more bent region of the spindle located in the mother cell (Figure 2C). Finally, in 29% of mitotic C377S *tub1* cells, abnormally long astral microtubules were observed. In contrast, no abnormally long astral microtubules were found in either *TUB1* or C214S *tub1* cells.

In wild-type cells, when a spindle elongates to approximately half the length of the mother cell, it translocates as a unit from the mother into the bud neck, and spindle elongation continues (Kahana *et al.*, 1995; Yeh *et al.*, 1995). In some C377S *tub1* cells, long spindles were positioned primarily in the mother (Figure 1, F and H), suggesting that this

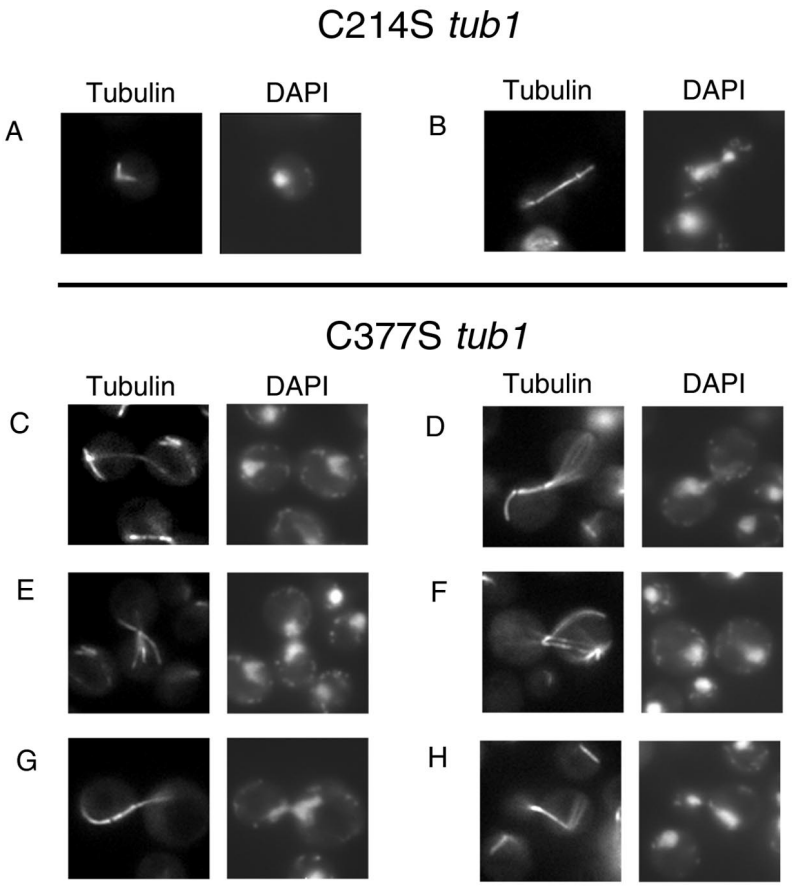

Percent of mitotic cells (30°C)

Strain	Normal microtubules	Long or misoriented astral microtubules	Long spindle microtubules
TUB1	100	0	0
C377S *tub1*	46	45	9
C214S *tub1*	88	12	0

Figure 1. Microtubule structures in C214S *tub1* and C377S *tub1* cells grown at 30°C. Cells were grown to log phase at 30°C, harvested, and processed for microscopy as described in MATERIALS AND METHODS. Microtubules were visualized by immunofluorescence staining of tubulin. Chromatin was visualized by DAPI staining. (A) C214S *tub1* cell in G1 phase of the cell cycle. (B) C214S *tub1* cell in M phase. (C–H) C377S *tub1* cells in M phase. At least 500 cells were counted for each strain. A summary of results for mitotic cells is shown in the accompanying table.

mutation may affect spindle translocation. To test this possibility, we selected mitotic cells with clearly separated chromosomes and determined the percentage of the spindle that had traversed the bud neck (Figure 3). In the majority of *TUB1* cells, chromosomes in the mother and bud were approximately equidistant from the bud neck. No *TUB1* cells were found with <30% of the spindle in the bud. In contrast, the majority of C377S *tub1* cells had spindles located primarily in the mother cell; values for C214S *tub1* cells were intermediate between *TUB1* and C377S *tub1* cells. Despite an apparent translocation defect, nuclei in C377S *tub1* cells were always found in both the mother and the bud suggesting that chromatin destined for the daughter cell was positioned far enough through the bud neck to prevent generation of anucleate cells. This conclusion is supported by the fact that no anucleate or multinucleate cells were observed in the C377S*tub1* strain.

Spindles with separated chromosomes were not always laterally centered in C377S *tub1* mutants (Figure 1G). As shown in Table 2, 44% of late anaphase C377S *tub1* cells had spindles that were not centered. This contrasts with *TUB1* cells in which 97% of the spindles are maintained in a more central position. A small percentage of C214S *tub1* cells (13%) displayed spindles that were not laterally centered.

Staining of actin filaments and cortical actin patches with rhodamine-phalloidin revealed no apparent differences be-

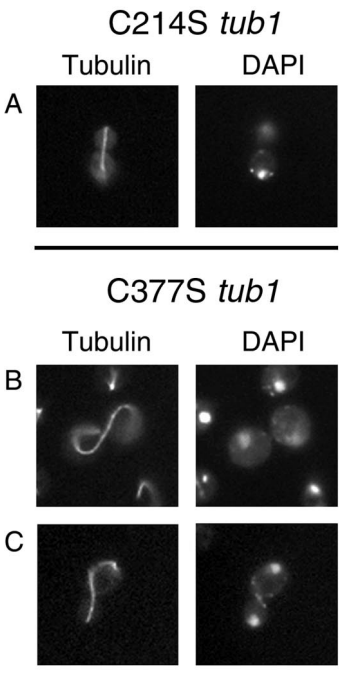

Percent of mitotic cells (15°C)

Strain	Normal microtubules	Long or misoriented astral microtubules	Long spindle microtubules
TUB1	100	0	0
C377S *tub1*	40	29	31
C214S *tub1*	94	0	6

Figure 2. Microtubule structures in mitotic C214S *tub1* and C377S *tub1* cells grown at 15°C. Cells were grown to log phase at 15°C, harvested, and processed for microscopy as described in MATERIALS AND METHODS. Microtubules were visualized by immunofluorescence staining of tubulin. Chromatin was visualized by staining with DAPI. (A) C214S *tub1* cell. (B and C) C377S *tub1* cells. At least 500 cells were counted for each strain. A summary of results for mitotic cells is shown in the accompanying table.

tween *TUB1*, C377S *tub1*, and C214S *tub1* cells. These data indicate that neither the C377S *tub1* nor C214S *tub1* mutation caused global damage to either the actin cytoskeleton or the actin-dependent polarity system in yeast.

Growth, Benomyl Sensitivity, and α-Tubulin Levels of Strains Expressing TUB1, C377S tub1, C241S tub1, or C214S/C377S tub1

Cold or temperature sensitivity is often used to select for α-tubulin mutants (Schatz *et al.*, 1988). To determine whether our *tub1* mutants displayed cold- and/or temperature-sensitive phenotypes, growth at 15, 30, and 37°C was examined. On YPD plates, the three *tub1* mutant strains grew as well as *TUB1* cells at all three temperatures, demonstrating that the mutations had no major effect on growth. To measure growth rates, cells were incubated in YPD medium at 15, 30, and 37°C, and at various time points, cells were counted. Again, no differences were found between the *tub1* mutants and *TUB1* cells. Doubling times for all four strains at 15, 30, and 37°C were 8.0, 1.6, and 2.0 h, respectively. These studies suggest that the *tub1* mutations did not affect the ability of α-tubulin to assemble into microtubules, a property of the protein that is exquisitely sensitive to conformational changes in the molecule (Sackett *et al.*, 1994).

Many tubulin mutations increase the amount of time cells spend in mitosis (Schatz *et al.*, 1988). The percentage of cells in mitosis is indicated by the percentage of large-budded cells within a population. With the use of phase contrast microscopy, we examined cells growing logarithmically in YPD medium, and counted those as large-budded if the bud was at least half the size of the mother. We found no significant differences in the percentage of large-budded cells between *TUB1* cells and the three *tub1* mutants at 15, 30, or 37°C. Examination of the overall size of both budded and unbudded cells revealed no differences between wild type and the mutants.

Increased sensitivity of cells to the anti-tubulin drug benomyl is a common phenotype of tubulin mutants (Schatz *et al.*, 1986, 1988, Richards *et al.*, 2000). We, therefore, compared sensitivity of *TUB1* cells and the three *tub1* mutant strains to different concentrations of the drug. As shown in Figure 4, the C377S *tub1* mutant displayed increased sensitivity to benomyl relative to *TUB1* cells, whereas the C214S *tub1* mutant was more resistant; the double mutant was intermediate between the two single mutants. The same relative sensitivities to benomyl were found when *TUB1* and *tub1* mutant cells were grown at 15°C. The level of α-tubulin in the three mutant strains was compared with that in *TUB1* cells by immunoblot analysis of whole cell extracts (Figure 5). Similar levels of α-tubulin were found in the *TUB1* and C377S *tub1* strains. However, both C214S *tub1* and C214S/C377S *tub1* cells contained ~30% more α-tubulin than *TUB1* cells. This increased level of α-tubulin protein in the C214S *tub1* strain may account for the increased benomyl resistance found in these cells relative to the *TUB1* strain; to our knowledge, benomyl resistance is the only phenotype associated with excess α-tubulin relative to β-tubulin (Schatz *et al.*, 1986). Likewise, increased α-tubulin expression in the double mutant may result in suppression of benomyl sensitivity that is found in the C377S *tub1* mutant.

In Vivo Palmitoylation of Wild-Type α-Tubulin in Yeast

Our previous studies suggest that cys-377 in Tub1p of *S. cerevisiae* may be posttranslationally modified by palmitoylation (Caron, 1997; Ozols and Caron, 1997). To determine whether wild-type α-tubulin in yeast is indeed palmitoylated in vivo, the following experiments were performed. Initially, we examined in vivo [^{3}H]palmitoylation of tubulin in haploids and diploids that produce wild-type levels of tubulin. However, we could not detect [^{3}H]palmitoylated tubulin within reasonable exposure times. This is most likely because *S. cerevisiae* contains relatively low levels of tubulin. For example, in platelets, where we were able to detect [^{3}H]palmitoylation of tubulin (Caron, 1997), tubulin comprises ~3% of the total protein (Steiner and Ikeda, 1979),

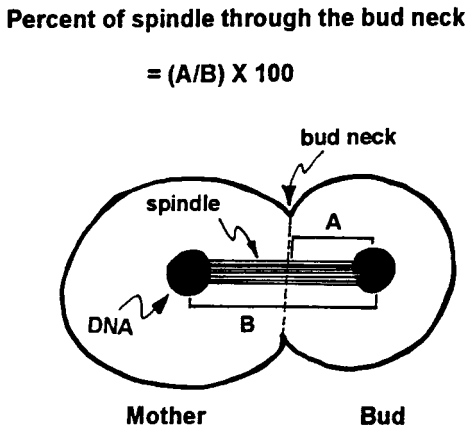

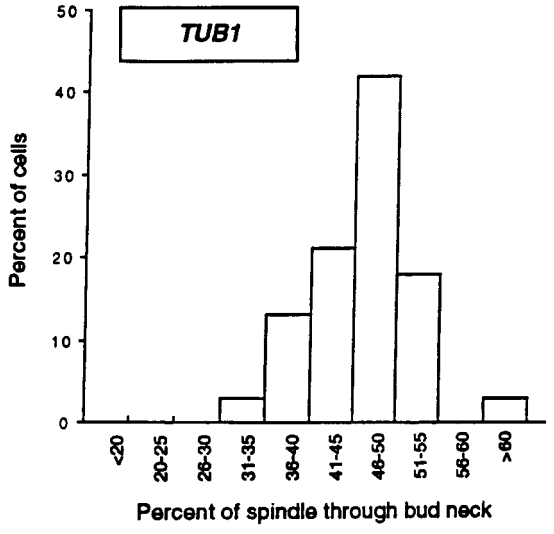

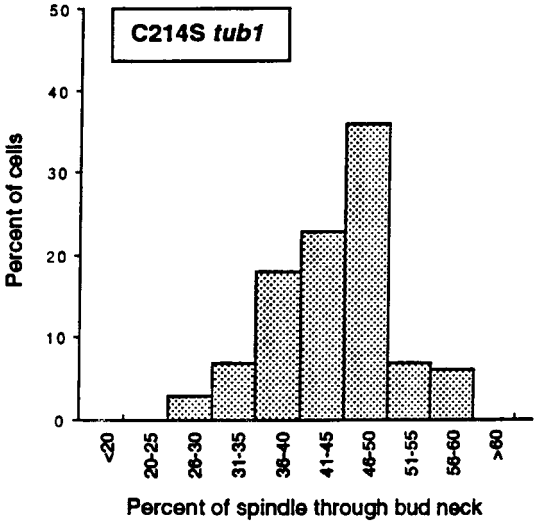

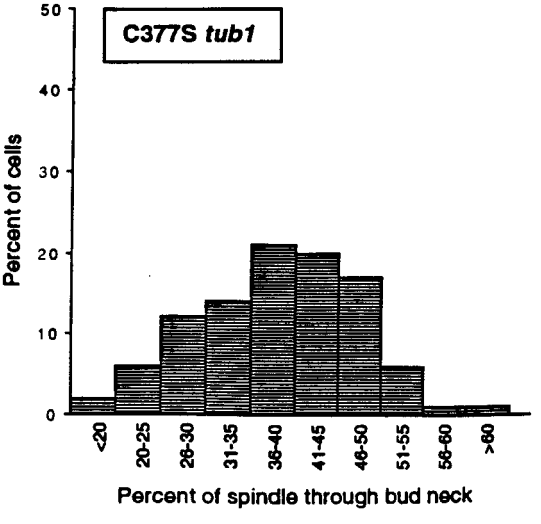

Figure 3. Percentage of anaphase spindle that traversed the bud neck. Cells were grown in YPD medium at 30°C to log phase, harvested, and fixed in ethanol (McMillan and Tatchell, 1994). DNA and bud scars were stained with DAPI and Calcofluor, respectively, and cells were examined by phase and fluorescence microscopy as described in MATERIALS AND METHODS. Random fields of cells were photographed. Cells in anaphase B (defined as mitotic cells with clearly separated DNA) were analyzed by measuring the distance between DNA in the mother and bud, and the distance between the bud neck (identified by phase microscopy and Calcofluor staining) and DNA in the bud. The mother and bud were differentiated by size, with the use of phase microscopy, and/or by Calcofluor staining. The percentage of the spindle that had traversed the bud neck was then determined. *TUB1* (n = 38), C377S *tub1* (n = 105), and C214S *tub1* (n = 73).

Table 2. Percent of cells with laterally centered spindles*

Position of duplicated nuclei	*TUB1*	C377S *tub1*	C214S *tub1*
Centered	97	56	87
Not centered	3	44	13

*Only mitotic cells with clearly separated chromatin were counted. Cells with duplicated nuclei resting along the sides of the cortex were counted as "not centered". All other cells were counted as "centered". Wild type (n = 39); C377S *tub1* (n = 90); C214S *tub1* (n = 64).

whereas in yeast only 0.05% of the protein is tubulin (Kilmartin, 1981). To circumvent this problem, we chose a diploid strain, FSY279, for biochemical analyses. This strain contains high copy galactose-inducible *TUB1* (α-tubulin) and *TUB2* (β-tubulin) overexpression plasmids (Weinstein and Solomon, 1990). After a 4-h induction with galactose, α- and β-tubulin levels increased by approximately five- and twofold, respectively, and a more extensive and dense array of microtubules formed. To decrease the level of endogenous palmitate, cells were preincubated with cerulenin (3 μg/ml) before addition of [^{3}H]palmitate (Mitchell *et al.*, 1994; Song and Dohlman, 1996). A time course study with strain FSY279 revealed maximal [^{3}H]palmitoylation of proteins after incubating cells with cerulenin for 4 h and adding [^{3}H]palmitate for the last hour.

To determine whether tubulin in strain FSY279 is [^{3}H]palmitoylated in vivo, cells were incubated in labeling medium containing 2% galactose to induce expression of tubulin (see MATERIALS AND METHODS). Analysis of whole cell extracts by 1D-PAGE revealed that several proteins were [^{3}H]palmitoylated and that the pattern of labeled proteins was distinct from that of Coomassie blue-stained proteins (Figure 6A). When α- and β-tubulin were immunoprecipitated from whole cell extracts, [^{3}H]palmitoylated α-tubulin was detected; a much weaker signal from [^{3}H]palmitoylated β-tubulin was also found (Figure 6B). Immunoblot analysis of immunoprecipitated proteins demonstrated that there was no cross-contamination of α- or β-tubulin in the immunoprecipitants.

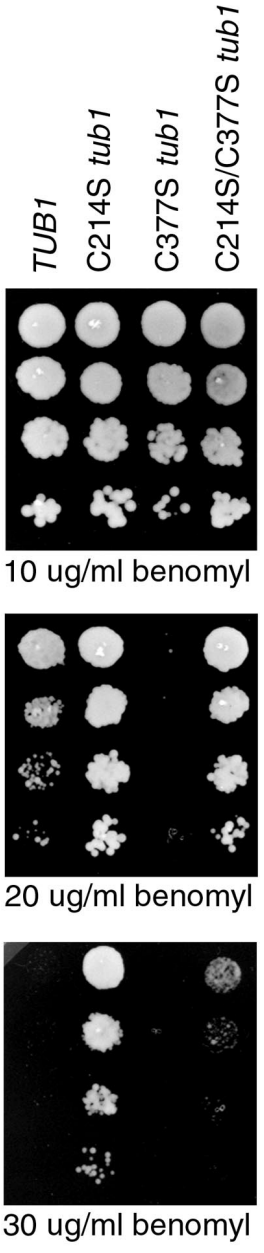

Figure 4. Benomyl sensitivity of *TUB1* and *tub1* strains. Serial dilutions of cells were spotted onto YPD plates containing 0–40 μg/ml benomyl. Cells grown on 10, 20, or 30 μg/ml benomyl at 25°C are shown.

In Vivo Palmitoylation of Tubulin from TUB1 and C377S tub1 Overexpressor Strains: Analysis of α-Tubulin Protein by Immunoprecipitation

Because cys-377 in *TUB1* may be a palmitoylation site (Ozols and Caron, 1997), we next sought to determine whether cys-to-ser mutation of this residue affected palmitoylation of the Tub1p in vivo. To this end, we constructed a diploid strain (JFY2705) that overexpresses C377S tub1p by approximately fivefold when cells are grown in the presence of galactose for 4 h (see MATERIALS AND METHODS). The rate and level of induction of α-tubulin in strain JFY2705 was similar to that in strain FSY279 (Figure 7).

To determine whether the C377S mutation affected the palmitoylation of α-tubulin, the *TUB1* (FSY279) and C377S *tub1* (JFY2705) overexpressor strains were incubated with galactose and [^{14}C]palmitate as described in MATERIALS AND METHODS. Cells were lysed and α-tubulin was immunoprecipitated. Duplicate samples of the immunopre-

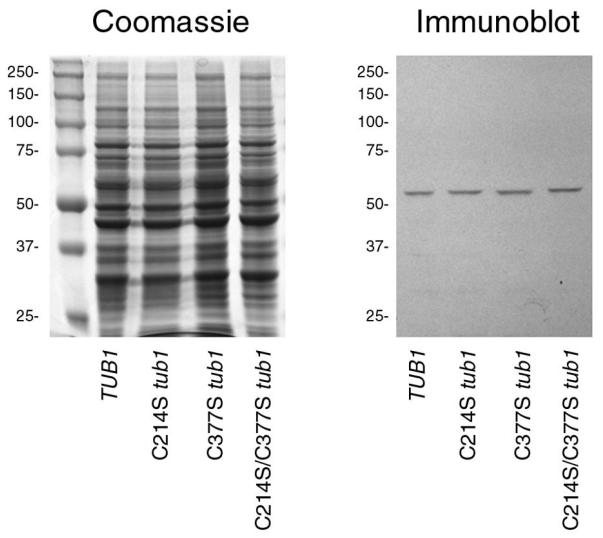

Figure 5. α-Tubulin levels in *TUB1* and *tub1* haploid strains. Cells were grown to log phase at 30°C, harvested, lysed, and processed for immunoblot analysis with anti-α-tubulin antibody as described in MATERIALS AND METHODS. Relative levels of α-tubulin were determined by scanning blots with an α-Innotech IS1000 Digital Imaging System and setting α-tubulin levels in the *TUB1* extract at 100%. Differences in protein loading onto SDS-PAGE gels were adjusted after scanning the corresponding Coomassie blue-stained gel. Molecular weight standards (kDa) are shown in the left lane.

cipitants were subjected to 1D-PAGE and immunoblot analysis with anti-α-tubulin antibody. As shown in Figure 8, in vivo palmitoylation of α-tubulin from the C377S mutant strain was reduced by ~50% compared with α-tubulin from the *TUB1* strain.

In Vivo Palmitoylation of Tubulin from TUB1 and C377S tub1 Overexpressor Strains: Analysis of α-Tubulin Protein by DEAE Chromatography

We next developed a second approach for analysis of palmitoylated tubulin that did not require immunoprecipitation of the protein. After incubation with galactose and [^{3}H]palmitate, tubulin was partially purified from both the *TUB1* (FSY279) and C377S *tub1* (JFY2705) overexpressor strains by DEAE chromatography as described in MATERIALS AND METHODS. DEAE fractions containing α-tubulin were identified by immunoblot analysis, pooled, and proteins were concentrated. Extracts were then processed for SDS-PAGE and either Coomassie blue staining and fluorography, or immunoblot analysis with anti-α-tubulin antibody.

As shown in Figure 9, similar patterns of Coomassie blue-stained proteins were found in DEAE extracts from *TUB1* and C377S *tub1* overexpressor strains. Tubulin in these extracts represented ~5% of the protein and was easily seen after SDS-PAGE and Coomassie blue staining. Because of this substantial enrichment of tubulin, we were able to analyze these fractions without immunoprecipitation.

Fluorography of the Coomassie blue-stained gels revealed similar patterns of [^{3}H]palmitoylated proteins between extracts from the two strains, but some differences in intensity

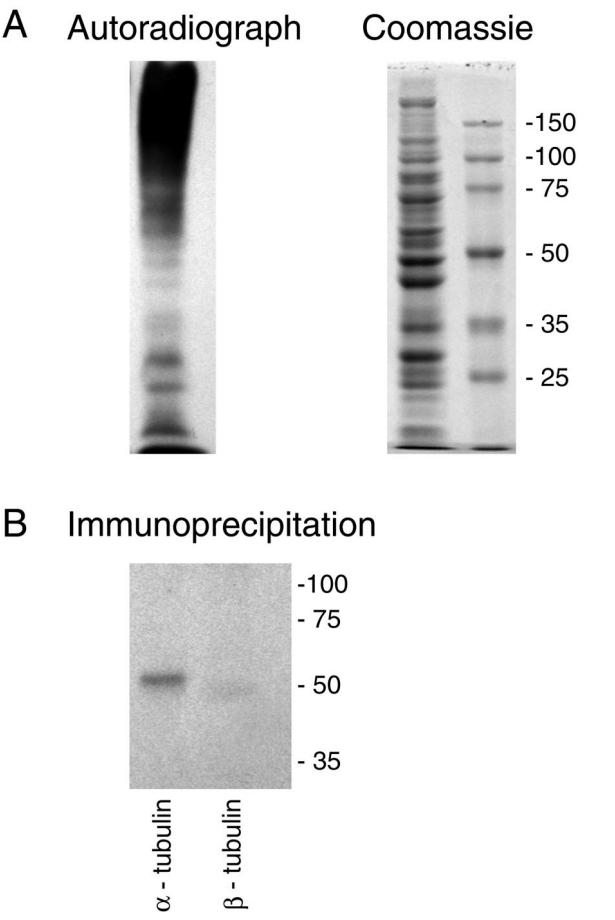

Figure 6. [^{3}H]Palmitoylation of tubulin in vivo. Overexpressor strain FSY279 (*TUB1*) was incubated with 2% galactose and [^{3}H]palmitate as described in MATERIALS AND METHODS. Cells were lysed and processed for immunoprecipitation of α- and β-tubulin. (A) Autoradiograph and corresponding Coomassie blue-stained gel of proteins from whole cell lysate after 1D-PAGE. Molecular weight markers (kDa) are shown on the right. (B) Autoradiograph of [^{3}H]palmitoylated protein immunoprecipitated with either anti-α-tubulin (left lane) or anti-β-tubulin (right lane) antibody.

were found (Figure 9). Examination of the tubulin band revealed [^{3}H]palmitoylated tubulin from the control strain (*TUB1*). However, the level of [^{3}H]palmitoylated tubulin in the C377S *tub1* strain was reduced by >60% of that in the control; immunoblot analysis of α-tubulin demonstrated that the *TUB1* and C377S *tub1* extracts contained similar levels of the protein (Figure 9).

DISCUSSION

Astral Microtubules and Nuclear Positioning Are Defective in Anaphase C377S tub1 Cells

Replacement of cys-377 with serine did not have global effects on microtubule-dependent functions, but instead resulted in an apparent anaphase-specific defect in astral microtubule functions.

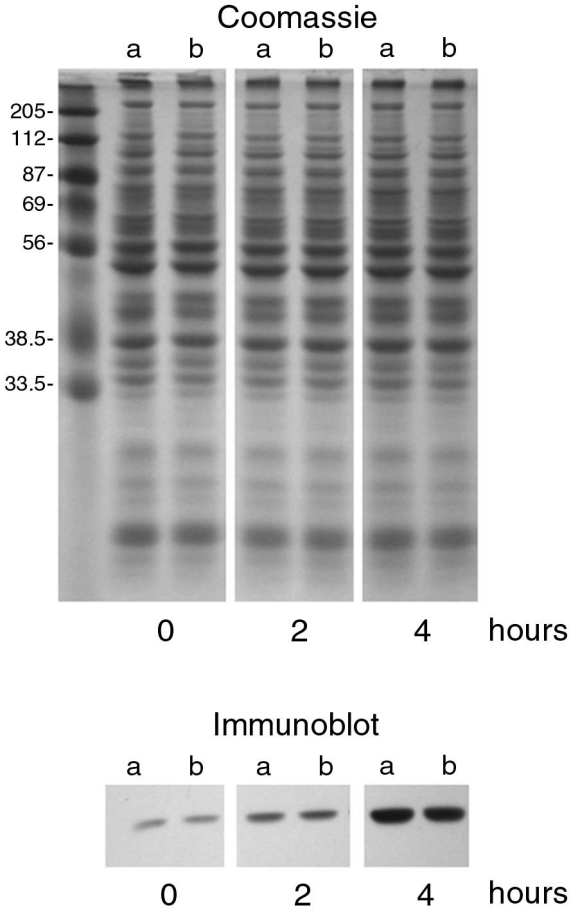

Figure 7. Induction of α-tubulin levels in *TUB1* and C377S *tub1* overexpressor strains. Strains FSY279 (*TUB1*) and JFY2705 (C377S *tub1*) were incubated with 2% galactose for up to 4 h. At several time points, cells were harvested, lysed, and processed for immunoblot analysis with anti-α-tubulin antibody. The corresponding Coomassie blue-stained gel is shown with molecular weight standards (kDa) in the left lane. (a) *TUB1*. (b) C377S *tub1*.

In *S. cerevisiae*, microtubules are involved in nuclear migration during mitosis and mating, and chromosome separation during cell division (Solomon, 1991). Recent studies, however, show that the role of microtubules in these processes is rather complex, being required at several specific times and for different reasons. Figure 10, A–G, is a compilation derived from those studies that have broadened our knowledge of the role of microtubules in *S. cerevisiae* (Jacobs *et al.*, 1988; Snyder *et al.*, 1991; Palmer *et al.*, 1992; Sullivan and Huffaker, 1992; McMillan and Tatchell, 1994; Farkasovsky and Küntzel, 1995; Kahana *et al.*, 1995; Yeh *et al.*, 1995; Doyle and Botstein, 1996; Waddle *et al.*, 1996; Shaw *et al.*, 1997; Carminati and Stearns, 1997; Miller and Rose, 1998; Goode *et al.*, 1999; Heil-Chapdelaine *et al.*, 1999; Tirnauer *et al.*, 1999; Adames and Cooper, 2000; Heil-Chapdelaine *et al.*, 2000; Yeh *et al.*, 2000; Farkasovsky and Küntzel, 2001).

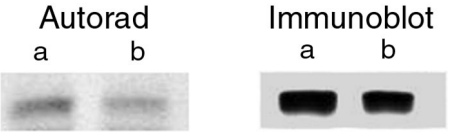

Figure 8. Effect of the C377S *tub1* mutation on in vivo palmitoylation of α-tubulin: use of immunoprecipitation. Overexpressor strains, FSY279 (*TUB1*) and JFY2705 (C377S *tub1*), were incubated with 2% galactose for 4 h; [^{14}C]palmitate for the last hour. Cells were lysed and extracts were processed for immunoprecipitation with anti-α-tubulin antibody as described in MATERIALS AND METHODS. Immunoprecipitants were subjected to 1D-PAGE followed by Coomassie blue staining and fluorography. A fraction (10%) of the immunoprecipitants was subjected to 1D-PAGE and processed for immunoblot analysis with anti-α-tubulin antibody. The autoradiograph shows [^{14}C]palmitoylated α-tubulin in *TUB1* (a) and C377S *tub1* (b) immunoprecipitants. The corresponding immunoblot shows α-tubulin levels in *TUB1* (a) and C377S *tub1* (b) immunoprecipitants.

Comparison of *TUB1* and C377S *tub1* haploid strains presented here suggests that astral microtubules do not require cys-377 during G1 phase of the cell cycle (Figure 10A), for positioning nuclei at emerging bud sites (Figure 10B) or for formation of mitotic spindles or alignment of spindles along the mother-bud axis (Figure 10C). However, striking differences were found between *TUB1* and C377S *tub1* cells during anaphase. First, in C377S *tub1* cells, correctly aligned

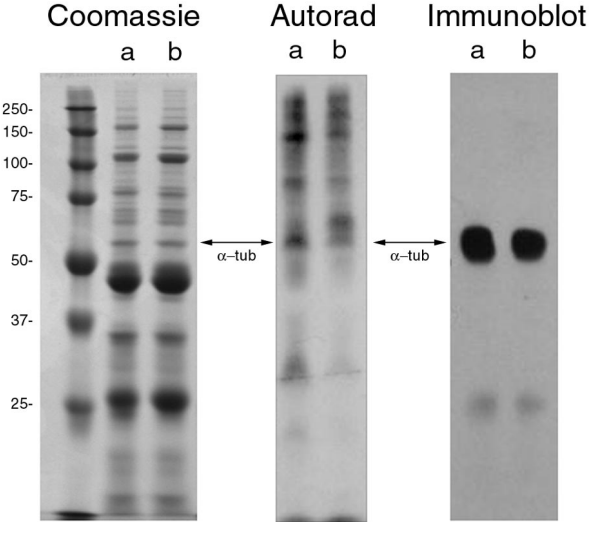

Figure 9. Effect of the C377S *tub1* mutation on in vivo palmitoylation of tubulin: use of DEAE chromatography. Overexpressor strains, FSY279 (*TUB1*) and JFY2705 (C377S *tub1*) were incubated with 2% galactose and [^{3}H]palmitate before cell lysis and DEAE chromatography (see MATERIALS AND METHODS). DEAE extracts containing α-tubulin were subjected to SDS-PAGE followed by Coomassie blue staining and fluorography. Duplicate samples were subjected to immunoblot analysis with anti-α-tubulin antibody. Molecular weight markers (kDa) are in the left lane of the Coomassie blue-stained gel. The position of α-tubulin is shown with an arrow. (a) *TUB1* extract. (b) C377S *tub1* extract.

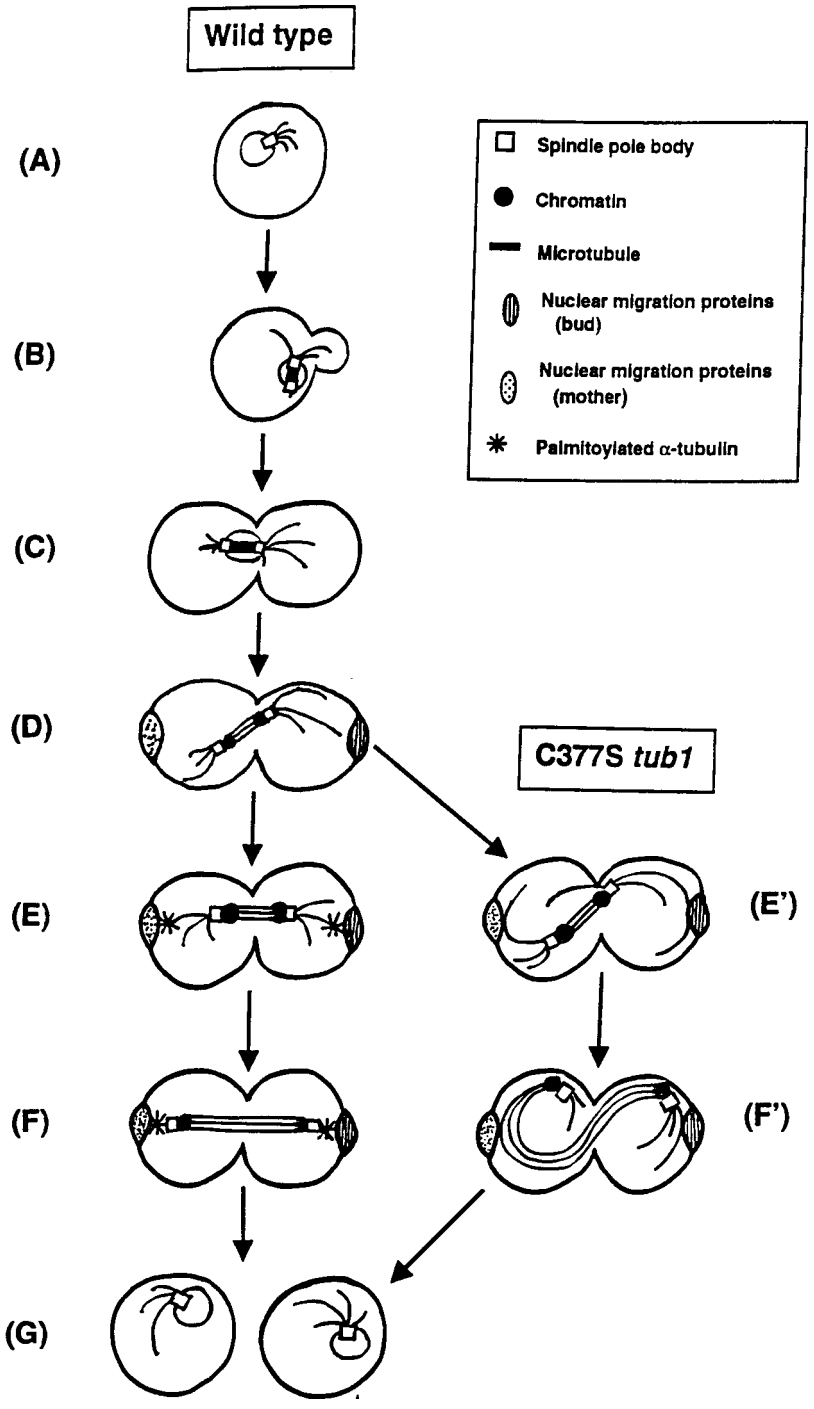

Figure 10. Schematic of microtubules in *TUB1* (wild-type) and C377S *tub1* cells during the yeast cell cycle and a model for the function of palmitoylated α-tubulin.

spindles were often found primarily in the mother cell (Figures 1 and 3), suggesting a role for cys-377 in the spindle translocation step (Figure 10E). Second, spindles and astral microtubules in late anaphase mutant cells were often found along the sides of cells (Table 2), suggesting that cys-377 plays a role in establishing and/or maintaining microtubule structures in a laterally centered position. Third, some astral microtubules in the mutant were misoriented, suggesting that cys-377 is involved in positioning or maintaining the position of astral microtubules. Fourth, upon reaching the cortex, astral microtubules in the mutant continued to grow resulting in abnormally long microtubules that curved around the periphery of the cell. This suggests that cys-377 plays a role in regulating astral microtubule length. Finally, the abnormally long mitotic spindles suggest that cys-377 plays a role in the termination of spindle elongation (Figure 10F).

Table 3. Summary of phenotypes from nuclear migration mutant and the C377S *tub1* mutant mitotic cells

Mutant protein	Increased benomyl sensitivity	Long or misoriented aMTs	Defect in spindle orientation	Defect in spindle translocation	Defect in lateral association of aMTs with cortex	Suggested locations of wild-type protein
dhc1p[a]	+	+	+	+	+	aMTs, SPB; cortex
arp1p/act5p[b]	+	+	+	+	+	Cortex
nlp100p[c]	nd	+	+	+	+	Bud SPB
jnm1p[d]	+	+	+	nd	+	Bud SPB, bud cortex tip; aMTs
num1p[e]	nd	+	+	+	+	Bud and mother cortex
kar9p[f]	+	+	+	+	nd	Bud cortex tip, aMTs
blm1p/yeb1p[g]	+	+	+	+	−	Bud cortex tip, distal ends of aMTs
crn1p[h]	+	+	−	nd	nd	Cortical actin patches
C377S tub1p[i]	+	+	−	+	−	NA

aMTs, astral microtubules; SPB, spindle pole body; +, mutation has effect; −, mutation has no apparent effect; nd, not determined; and NA, not applicable.

[a] Li *et al.* (1993), Eshel *et al.* (1993), Yeh *et al.* (1995), Carminati and Stearns (1997), Shaw *et al.* (1997), Miller and Rose (1998).

[b] Muhua *et al.* (1994), Clark and Meyer (1994), Adames and Cooper (2000).

[c] Kahana *et al.* (1998).

[d] McMillan and Tatchell (1994).

[e] Kormanec *et al.* (1991), Farkasovsky and Küntzel (1995), Heil-Chapdelaine *et al.* (2000), Farkasovsky and Küntzel (2001).

[f] Miller and Rose (1998), Miller *et al.* (1999), Korinek *et al.* (2000), Lee *et al.* (2000).

[g] Schwartz *et al.* (1997), Tirnauer *et al.* (1999), Adames and Cooper (2000), Korinek *et al.* (2000), Lee *et al.* (2000).

[h] Heil-Chapdelaine *et al.* (1998), Goode *et al.* (1999).

[i] This article.

Similarity of C377S tub1 Mutant with Nuclear Migration Mutations

Mutation of several nontubulin proteins that are involved in mitotic nuclear migration (Dhc1, Arp1p/Act5p, Nip100p, Jnm1p, Num1p, Kar9p, Bim1p/Yeb1p, Crn1p) results in remarkably similar phenotypes to those described for the C377S α-tubulin mutant. As with the C377S *tub1* mutant, mutation of these nuclear migration proteins has little or no effect on cell growth at different temperatures (Kormanec *et al.*, 1991; Eshel *et al.*, 1993; Li *et al.*, 1993; McMillan and Tatchell, 1994; Muhua *et al.*, 1994; Kahana *et al.*, 1998; Goode *et al.*, 1999). However, phenotypes resulting from these mutations are mitosis specific. Like the C377S *tub1* mutant, nuclear migration protein mutations show incomplete penetrance of phenotypes: the percentage of cells affected by the different nuclear migration mutations varies from 4 to 50%, depending on the phenotype and the temperature of growing cultures. A comparison of phenotypes in nuclear migration mutants and in the C377S *tub1* mutant is shown in Table 3. In wild-type cells, distal ends of astral microtubules appear to intersect with Bim1p/Yeb1p, Kar9p and Jnm1p that concentrate at the tip of the bud cortex in large-budded cells (McMillan and Tatchell, 1994; Miller and Rose, 1998; Miller *et al.*, 1999; Tirnauer *et al.*, 1999; Adames and Cooper, 2000; Korinek *et al.*, 2000; Lee *et al.*, 2000). It was suggested that these proteins assist in the tethering of astral microtubules to this region of the bud cortex during anaphase. Num1p localizes to the cortex of the mother and the bud where it is also thought to tether astral microtubules (Farkasovsky and Küntzel, 1995; Heil-Chapdelaine *et al.*, 2000; Farkasovsky and Küntzel, 2001). Arp1p/Act5p (Clark and Meyer, 1994; Muhua *et al.*, 1994; Adames and Cooper, 2000), an *S. cerevisiae*-specific actin-related protein, and Nip100p (Kahana *et al.*, 1998), the yeast homolog of p150^{glued}, are components of dynactin complex, which is required for dynein-mediated vesicle transport (Gill *et al.*, 1991; Schroer and Sheetz, 1991). Dhc1p is the dynein heavy chain in *S. cerevisiae*. In a review of the function of dynactin and dynein, Schroer (1994) suggests that dynactin complex associates with the cell cortex and binds to dynein which, in turn, links astral microtubules to the cortex. Although Nip100p has so far only been localized to bud-directed spindle pole bodies (Kahana *et al.*, 1998), Arp1p/Act5p and dynein have been localized to the cortex of mitotic cells (Adames and Cooper, 2000). Furthermore, dynein/dynactin complex is required for the lateral associations of astral microtubules with the cortex. A model is presented by Adames and Cooper (2000) in which dynein/dynactin complex, anchored to the cortex, binds the sides of astral microtubules and walks in the minus (or spindle pole body) end direction, thereby generating the large force needed to pull the nucleus into the bud neck during anaphase.

Finally, Crn1p is a highly conserved actin binding protein whose activity may intersect with that of cys-377 of α-tubulin. As an abundant component of cortical actin patches, Crn1p may link the actin and microtubule cytoskeletons in yeast (Heil-Chapdelaine *et al.*, 1998; Goode *et al.*, 1999). *crn1*Δ strains show no defects in growth rates, and normal actin cables are maintained. However, cortical actin patches are absent. Interestingly, like C377S *tub1* cells, *crn1*Δ mutants display excessively long and misoriented astral microtubules during anaphase (5% of the population), but no mi-

sorientation of spindles. This suggests the possibility that Crn1p in cortical patches (which localize to the bud tip during mitosis) may help to guide astral microtubules to the cortex of the bud tip. A similar actin-mediated guidance mechanism for microtubule–plasma membrane interactions is described for vertebrate cells (Kaverina *et al.*, 1998).

In Vivo Palmitoylation of Tubulin in Yeast

In addition to its effect on mitotic astral microtubules, cys-to-ser mutagenesis of cys-377 resulted in a substantial decrease (50–62%) in the in vivo palmitoylation of yeast α-tubulin (Figures 8 and 9), suggesting that this cysteine residue is a site of palmitoylation. This level of reduction is found in many palmitoylated proteins with single amino acid mutations (Druey *et al.*, 1999). The residual label in yeast tubulin may be due to palmitoylation of an unknown secondary site in α-tubulin. Alternatively, the presumptive secondary site identified in porcine brain α-tubulin (Caron and Ozols, 1997) may be palmitoylated in yeast α-tubulin. However, the microtubule and nuclear migration phenotype of the double mutant (C214S/C377S *tub1*) was equivalent to the single mutant (C377S *tub1*), making unclear the functional significance of cys-214 as a secondary palmitoylation site, if it is one. A third possibility for residual label is palmitoylation of Tub3p; unlike the haploid strains used for phenotypic analysis, *TUB3* was not deleted in the *TUB1* and C377S *tub1* diploid overexpressor strains used for biochemical studies. However, detection of palmitoylated Tub3p seems unlikely because this protein was expressed at 20-fold lower levels compared with C377S tub1p; in support of this conclusion, we note again that palmitoylation of Tub1p was not detected in the diploid strain without the galactose-induced fivefold increase in expression of the protein. Finally, under our immunoprecipitation conditions, β-tubulin is not immunoprecipitated with anti-α-tubulin antibody (Caron *et al.*, 1985; Caron, unpublished data). Therefore, residual label found after immunoprecipitation of α-tubulin from C377S *tub1* extracts (Figure 8) is not due to palmitoylation of Tub2p.

In support of cys-377 as a primary site of palmitoylation of Tub1p, tubulin partially purified from strain FSY279 (*TUB1*) was [^{3}H]palmitoylated in our cell-free system (Caron, 1997), whereas tubulin from strain JFY2705 (C377S *tub1*) was not (Caron, unpublished data). This cell-free system has been shown to palmitoylate the same sites in nontubulin proteins as found in vivo (Druey *et al.*, 1999).

Model for Function of Palmitoylated α-Tubulin

In eukayotic cells, including *S. cerevisiae*, the long-chain fatty acid palmitate is covalently linked to cysteine residues via thioester bonds (reviewed in Bizzozero *et al.*, 1994; Casey, 1995; Mumby, 1997). The reversibility of this modification suggests that palmitoylation regulates membrane activities. For example, palmitoylation results in the sequestration of some proteins, such as nitric-oxide synthase (Garcia-Cardena *et al.*, 1996; Shaul *et al.*, 1996) and proteins involved in T-cell receptor signaling (Zhang *et al.*, 1998), within membrane microdomains. Palmitoylation also determines protein–protein interactions within the membrane. For example, palmitoylation of the β-adrenergic receptor prevents its phosphorylation by cAMP-dependent protein kinase C, which in turn reduces its ability to interact with Gs protein (Moffett *et al.*, 1996).

α- and β-Tubulin are palmitoylated in resting human platelets, and the level of palmitoylated tubulin decreases when platelets are activated with thrombin (Caron, 1997). This depalmitoylation of tubulin coincides with thrombin-induced disassembly of the peripheral band of microtubules juxtaposed to the cell cortex.

The phenotype of the C377S *tub1* mutant is consistent with the hypothesis that palmitoylation of cys-377 plays a role in static microtubule–cortex interactions. First, the astral microtubule defects associated with this mutation occur during the same period of the cell cycle (anaphase B) in which static astral microtubule–cortex interactions occur (Carminati and Stearns, 1997; Shaw *et al.*, 1997; Adames and Cooper, 2000). Other microtubule–cortex interactions occur earlier in mitosis, but these are not static (Shaw *et al.*, 1997). As suggested by Shaw *et al.* (1997), these early, transient microtubule–cortex interactions may correct errors in bud site selection and spindle orientation. Second, astral microtubules in the C377S *tub1* mutant do not interact with the bud tip of the cortex the same way that they do in *TUB1* cells: instead of stopping at the bud tip, astral microtubules in the mutant continue to grow. Such a phenotype is consistent with a mutation that alters the affinity of α-tubulin for membranes. Third, phenotypes associated with the C377S *tub1* mutant are strikingly similar to those from a class of nuclear migration proteins whose functions involve microtubule–cortex interactions.

A simple "lock and key" model (Figure 10) for the function of palmitoylated α-tubulin accommodates microtubule phenotypes observed in the C377S *tub1* mutant as well as data on nuclear migration proteins and known functions of astral microtubules. As wild-type cells enter anaphase and astral microtubules lengthen, these microtubules associate laterally with the cortex of both the mother and bud via interactions with cortical-anchored dynein/dynactin complex (Adames and Cooper, 2000). Through these interactions, astral microtubules slide along the cortex, pulling the spindle into the bud neck (Figure 10D). On reaching the cortical tips, astral microtubules probe the surface for a specific region that contains nuclear migration proteins (i.e., Crn1p, Bim1p/Yeb1p, Kar9p, Jnm1p, Num1p) and palmitoylating enzymes. Through interactions with these proteins, α-tubulin at or near the plus (or cortex) end of these microtubules is palmitoylated, which in turn locks the microtubule end onto the cortex. This tethering of the microtubule inhibits further microtubule assembly at its plus end and leads to the more static and rigid structure that is found during this stage of mitosis (Palmer *et al.*, 1992; Carminati and Stearns, 1997; Shaw *et al.*, 1997). Because the tethered microtubules (and attached spindle) are "locked" into a specific position, they assist in translocating the spindle through the bud neck and maintaining the spindle in a laterally centered position (Figure 10E). Once the spindle has elongated to the length of the cell, the shortened and tethered astral microtubules prevent further elongation (Figure 10F). Finally, α-tubulin is depalmitoylated, the spindle disassembles, nuclei become centered in the mother and bud, and cytokinesis occurs (Figure 10G).

Microtubule–cortex interactions are also found in higher eukaryotes. As in *S. cerevisiae*, dynein/dynactin complex has

been localized to cortical–microtubule attachment sites in *Caenorhabditis elegans* (Hyman and White, 1987; Hyman, 1989; Skop and White, 1998). Here, these interactions are required for asymmetric cell division during embryogenesis, which in turn leads to the polarization of cellular components and the generation of cell diversity (Gönczy and Hyman, 1996; reviewed in White and Strome, 1996). Microtubule–cortex interactions during cell division may be more important for the survival of higher eukaryotes than *S. cerevisiae*: unlike *S. cerevisiae*, the site of cytokinesis in higher eukaryotes is determined by the position of the mitotic spindle. It is possible that palmitoylation of α-tubulin plays a role in establishing or maintaining static microtubule–cortex interactions required for the correct positioning of nuclei during cell division of higher eukaryotes.

ACKNOWLEDGMENTS

This study is dedicated to the memory of Lea Economos. We thank Richard Berlin, Jane Caron, Sue Cavar, Peter Deckers, Gary Hunnicutt, Tim Hla, Stephen King, Frank Morgan, Susan Naide, Susan Preston, Pramod Svrivastava, and members of the Solomon laboratory for suggestions and comments. J.M.C. thanks members of CBIT for help with the microscopy; Elizabeth Caron for help with the growth rate studies; and gratefully acknowledges Peter Deckers, Susan Preston, and Richard Berlin for continued support. This work was supported by grants from Lea's Foundation for Leukemia Research, Inc., and the American Heart Association, Heritage Affiliate, Inc., to J.M.C., and a grant from the National Institute of General Medical Sciences to F.S.

REFERENCES

Adames, N.R., and Cooper, J.A. (2000) Microtubule interactions with the cell cortex causing nuclear movements in *Saccharomyces cerevisiae*. J. Cell Biol. *149*, 863–874.

Barnes, G., Louie, K.A., and Botstein, D. (1992). Yeast proteins associated with microtubules in vitro and in vivo. Mol. Biol. Cell *3*, 29–47.

Bizzozero, O.A., Tetzloff, S.U., and Bharadwaj, M. (1994). Overview: protein palmitoylation in the nervous system: current views and unsolved problems. Neurochem. Res. *19*, 923–933.

Boeke, J.D., LaCroute, F., and Fink, G.R. (1984). A positive selection for mutants lacking orotidine-5′-phosphate decarboxylase activity in yeast: 5-fluoro-orotic acid resistance. Mol. Gen. Genet. *197*, 345–347.

Boeke, J.D., Trueheart, J., Natsoulis, G., and Fink, G.R. (1987). 5-Fluoroorotic acid as a selective agent in yeast molecular genetics. Methods Enzymol. *154*, 164–175.

Carminati, J.L., and Stearns, T. (1997). Microtubules orient the mitotic spindle in yeast through dynein-dependent interactions with the cell cortex. J. Cell Biol. *138*, 629–641.

Caron, J.M. (1997). Posttranslational modification of tubulin by palmitoylation: in vivo and cell-free studies. Mol. Biol. Cell *8*, 621–636.

Caron, J.M., Jones, A.L., and Kirschner, M.W. (1985). Autoregulation of tubulin synthesis in hepatocytes and fibroblasts. J. Cell Biol. *101*, 1763–1772.

Casey, P. (1995). Protein lipidation in cell signaling. Science *268*, 221–225.

Clark, S.W., and Meyer, D.I. (1994). *ACT3*: a putative centractin homologue in *S. cerevisiae* is required for proper orientation of the mitotic spindle. J. Cell Biol. *127*, 129–138.

Doyle, T., and Botstein, D. (1996). Movement of yeast cortical actin cytoskeleton visualized *in vivo*. Proc. Natl. Acad. Sci. USA *93*, 3886–3891.

Druey, K.M., Yazar-Ugur, O., Caron, J.M., Chen, C.K., Backlund, P.S., and Jones, T.L.Z. (1999). Amino-terminal cysteine residues of RGS16 are required for palmitoylation and modulation of Gi and Gq-mediated signaling. J. Biol. Chem. *274*, 18836–18842.

Eshel, D., Urrestarazu, L.A., Vissers, S., Jauniaux, J.-C., van Vliet-Reedijk, J.C., Planta, R.J., and Gibbons, I.R. (1993). Cytoplasmic dynein is required for normal nuclear segregation in yeast. Proc. Natl. Acad. Sci. USA *90*, 11172–11176.

Farkasovsky, M., and Küntzel, H. (1995). Yeast Num1p associates with the mother cell cortex during S/G2 phase and affects microtubular functions. J. Cell Biol. *131*, 1003–1014.

Farkasovsky, M., and Küntzel, H. (2001). Cortical Num1p interacts with the dynein intermediate chain *Pac*I1p, and cytoplasmic microtubules in budding yeast. J. Cell Biol. *152*, 251–262.

Funabashi, H., Kawaguchi, A., Tomoda, H., Omura, S., Okuda, S., and Iwasaki, S. (1989). Binding site of cerulenin in fatty acid synthetase. J. Biochem. *105*, 751–755.

Garcia-Cardena, G., Oh, P., Liu, J., Schnitzer, J.E., and Sessa, W.C. (1996). Targeting of nitric oxide synthase to endothelial cell caveolae via palmitoylation: implications for nitric oxide synthase signaling. Proc. Natl. Acad. Sci. USA *93*, 6448–6453.

Gill, S.R., Schroer, T.A., Szilak, I., Steuer, E.R., Sheetz, M.P., and Cleveland, D.W. (1991). Dynactin, a conserved, ubiquitously expressed component of an activator of vesicle motility mediated by cytoplasmic dynein. J. Cell Biol. *115*, 1639–1650.

Gönczy, P., and Hyman, A.A. (1996). Cortical domains and the mechanism of asymmetric cell division. Trends Cell Biol. *6*, 382–387.

Goode, B.L., Wong, J.J., Butty, A.C., Peter, M., McCormack, A.L., Yates, J.R., Drubin, D.G., and Barnes, G. (1999). Coronin promotes the rapid assembly and cross-linking of actin filaments and may link the actin and microtubule cytoskeletons in yeast. J. Cell Biol. *144*, 83–98.

Heil-Chapdelaine, R.A., Tran, N.K., and Cooper, J.A. (1998). The role of *Saccharomyces cerevisiae* coronin in the actin and microtubule cytoskeletons. Curr. Biol. *19*, 1281–1284.

Heil-Chapdelaine, R.A., Adames, N.R., and Cooper, J.A. (1999). Formin' the connection between microtubules and the cell cortex. J. Cell Biol. *144*, 809–811.

Heil-Chapdelaine, R.A., Oberle, J.R., and Cooper, J.A. (2000). The cortical protein Num1p is essential for dynein-dependent interactions of microtubules with the cortex. J. Cell Biol. *151*, 1337–1343.

Hyman, A.A. (1989). Centrosome movement in the early divisions of *Caenorhabditis elegans*: a cortical site determining centrosome position. J. Cell Biol. *109*, 1185–1193.

Hyman, A.A., and White, J.G. (1987). Determination of cell division axes in the early embryogenesis of *Caenorhabditis elegans*. J. Cell Biol. *105*, 2123–2135.

Jacobs, C.W., Adams, A.E.M., Szaniszlo, P.J., and Pringle, J.R. (1988). Functions of microtubules in the *Saccharomyces cerevisiae* cell cycle. J. Cell Biol. *107*, 1409–1426.

Kahana, J.A., Schlenstedt, G., Evanchuk, D.M., Geiser, J.R., Hoyt, M.A., and Silver, P.A. (1998). The yeast dynactin complex is involved in partitioning the mitotic spindle between mother and daughter cells during anaphase B. Mol. Biol. Cell *9*, 1741–1756.

Kahana, J.A., Schnapp, B.J., and Silver, P.A. (1995). Kinetics of spindle pole body separation in budding yeast. Proc. Natl. Acad. Sci. USA *92*, 9707–9711.

Kaverina, I., Rottner, K., and Small, J.V. (1998). Targeting, capture, and stabilization of microtubules at early focal adhesions. J. Cell Biol. *142*, 181–190.

Kilmartin, J. (1981). Purification of yeast tubulin by self-assembly in vitro. Biochemistry *20*, 3629–3633.

Korinek, W.S., Copeland, M.J., Chaudhuri, A., and Chant, J. (2000). Molecular linkage underlying microtubule orientation toward cortical sites in yeast. Science *287*, 2257–2259.

Kormanec, J., Schaaff-Gerstenschläger, I., Zimmermann, F.K., Perecko, D., and Küntzel, H. (1991). Nuclear migration in *Saccharomyces cerevisiae* is controlled by the highly repetitive 313 kDa NUM1 protein. Mol. Gen. Genet. *230*, 277–287.

Laemmli, U.K. (1970). Cleavage of structural proteins during assembly of the head of bacteriophage T4. Nature *227*, 680–685.

Lee, L., Tirnauer, J.S., Junjun, L., Schuyler, S.C., Liu, J.Y., and Pellman, D. (2000). Positioning of the mitotic spindle by a cortical-microtubule capture mechanism. Science *287*, 2260–2262.

Li, Y.-Y., Yeh, E., Hays, T., and Bloom, K. (1993). Disruption of mitotic spindle orientation in a yeast dynein mutant. Proc. Natl. Acad. Sci. USA *90*, 10096–10100.

McMillan, J.N., and Tatchell, K. (1994). The *JNM1* gene in the yeast *Saccharomyces cerevisiae* is required for nuclear migration and spindle orientation during the mitotic cell cycle. J. Cell Biol. *125*, 143–158.

Miller, R.K., Matheos, D., and Rose, M.D. (1999). The cortical localization of the microtubule orientation protein, Kar9p, is dependent upon actin and proteins required for polarization. J. Cell Biol. *144*, 963–975.

Miller, R.K., and Rose, M.D. (1998). Kar9p is a novel cortical protein required for cytoplasmic microtubule orientation in yeast. J. Cell Biol. *140*, 377–390.

Mitchell, D.A., Farh, L., Marshall, T.K., and Deschenes, R.J. (1994). A polybasic domain allows nonprenylated Ras proteins to function in *Saccharomyces cerevisiae*. J. Biol. Chem. *269*, 21540–21546.

Moffett, S., Adams, L., Bonin, H., Loisel, T.P., Bouvier, M., and Mouillac, B. (1996). Palmitoylated cysteine 341 modulates phosphorylation of the β2-adrenergic receptor by the cAMP-dependent protein kinase. J. Biol. Chem. *271*, 21490–21497.

Muhua, L., Karpova, T.S., and Cooper, J.A. (1994). A yeast actin-related protein homologous to that in vertebrate dynactin complex is important for spindle orientation and nuclear migration. Cell *78*, 669–679.

Mumby, S.M. (1997). Reversible palmitoylation of signaling proteins. Curr. Opin. Cell Biol. *9*, 148–154.

Ozols, J., and Caron, J.M. (1997). Posttranslational modification of tubulin by palmitoylation: identification of sites of palmitoylation. Mol. Biol. Cell *8*, 637–645.

Palmer, R.E., Sullivan, D.S., Huffaker, T., and Koshland, D. (1992). Role of astral microtubules and actin in spindle orientation and migration in the budding yeast. *Saccharomyces cerevisiae*. J. Cell Biol. *119*, 583–593.

Powers, S., Michaelis, S., Broek, D., Santa Anna, S., Field, J., Herskowitz, I., and Wigler, M. (1986). *RAM*, a gene of yeast required for a functional modification of *RAS* proteins and for production of mating pheromome a-factor. Cell *47*, 413–422.

Richards, K.L., Anders, K.R., Nogales, E., Schwartz, K., Downing, K.N., and Botstein, D. (2000). Structure-function relationships in yeast tubulins. Mol. Biol. Cell *11*, 1887–1903.

Rose, M.D., Winston, F., and Hieter, P. (1990). Methods in Yeast Genetics: A Laboratory Course Manual, Cold Spring Harbor, NY: Cold Spring Harbor Laboratory Press.

Sackett, D.L., Bhattacharyya, B., and Wolff, J. (1994). Local unfolding and the stepwise loss of the functional properties of tubulin. Biochemistry *33*, 12868–12878.

Schatz, P.J., Georges, G.E., Solomon, F., and Botstein, D. (1987). Insertions of up to 17 amino acids into a region of α-tubulin do not disrupt function in vivo. Mol. Cell. Biol. *7*, 3799–3805.

Schatz, R.J., Solomon, F., and Botstein, D. (1986). Genetically essential and nonessential α-tubulin genes specify functionally interchangeable proteins. Mol. Cell. Biol. *6*, 3722–3733.

Schatz, P.J., Solomon, F., and Botstein, D. (1988). Isolation and characterization of conditional-lethal mutations in the *TUB1* α-tubulin gene of the yeast *Saccharomyces cerevisiae*. Genetics *120*, 681–695.

Schroer, T.A. (1994). New insights into the interaction of cytoplasmic dynein with the actin-related protein, Arp1. J. Cell Biol. *127*, 1–4.

Schroer, T.A., and Sheetz, M.P. (1991). Two activators of microtubule-based vesicle transport. J. Cell Biol. *115*, 1309–1318.

Schwartz, K., Richards, K., and Botstein, D. (1997). BIM1 encodes a microtubule-binding protein in yeast. Mol. Biol. Cell *8*, 2677–2691.

Shaul, P.W., Smart, E.J., Robinson, L.J., German, Z., Yuhanna, I.S., Ying, Y., Anderson, R.G.W., and Michel, T. (1996). Acylation targets endothelial nitric oxide synthase to plasmalemmal caveolae. J. Biol. Chem. *271*, 6518–6522.

Shaw, S.L., Yeh, E., Maddox, P., Salmon, E.D., and Bloom, K. (1997). Astral microtubule dynamics in yeast: a microtubule-based searching mechanism for spindle orientation and nuclear migration into the bud. J. Cell Biol. *139*, 985–994.

Skop, A.R., and White, J.G. (1998). The dynactin complex is required for cleavage plane specification in early *Caenorhapditis elegans* embryos. Curr. Biol. *8*, 1110–1116.

Snyder, M., Gehrung, S., and Page, B.D. (1991). Studies concerning the temporal and genetic control of cell polarity in *Saccharomyces cerevisiae*. J. Cell Biol. *114*, 515–532.

Solomon, F. (1991). Analyses of the cytoskeleton in *Saccharomyces cerevisiae*. Annu. Rev. Cell Biol. *7*, 633–662.

Solomon, F., Connell, L., Kirkpatrick, D., Praitis, V., and Weinstein, B. (1992). Methods for studying the yeast cytoskeleton. In: The Cytoskeleton, ed. K. Carraway and C. Carraway, Oxford, UK: Oxford University Press, 197–222.

Song, J., and Dohlman, H.G. (1996). Partial constitutive activation of pheromone responses by a palmitoylation-site mutant of a G protein α subunit in yeast. Biochemistry *35*, 14806–14817.

Steiner, M., and Ikeda, Y. (1979). Quantitative assessment of polymerized and depolymerized platelet microtubules—changes caused by aggregating agents. J. Clin. Invest. *63*, 443–448.

Sullivan, D.S., and Huffaker, T.C. (1992). Astral microtubules are not required for anaphase B in *Saccharomyces cerevisiae*. J. Cell Biol. *119*, 379–388.

Tirnauer, J.S., O'Toole, E., Berrueta, L., Bierer, B.E., and Pellman, D. (1999). Yeast Bim1p promotes the G1-specific dynamics of microtubules. J. Cell Biol. *145*, 993–1007.

Vega, L.R., Fleming, J., and Solomon, F. (1998). An α-tubulin mutant destabilizes the heterodimer: phenotypic consequences and interactions with tubulin-binding proteins. Mol. Biol. Cell *9*, 2349–2360.

Waddle, J.A., Karpova, T.S., Waterston, R.H., and Cooper, J.A. (1996). Movement of cortical actin patches in yeast. J. Cell Biol. *132*, 861–870.

Weinstein, B., and Solomon, F. (1990). Phenotypic consequences of tubulin overproduction in *Saccharomyces cerevisiae*: differences between alpha-tubulin and beta-tubulin. Mol. Cell. Biol. *10*, 5295–5304.

Wessel, D., and Flügge, U.I. (1984). A method for the quantitative recovery of protein in dilute solution in the presence of detergents and lipids. Anal. Biochem. *138*, 141–143.

White, J., and Strome, S. (1996). Cleavage plane specification in *C. elegans*: how to divide the spoils. Cell *84*, 195–198.

Yeh, E., Skibbens, R.V., Cheng, J.W., Salmon, E.D., and Bloom, K. (1995). Spindle dynamics and cell cycle regulation of dynein in the budding yeast *Saccharomyces cerevisiae*. J. Cell Biol. *130*, 687–700.

Yeh, E., Yang, C., Chin, E., Maddox, P., Salmon, E.D., Lew, D.J., and Bloom, K. (2000). Dynamic positioning of mitotic spindles in yeast. role of microtubule motors and cortical determinants. Mol. Biol. Cell *11*, 3949–3961.

Zhang, W., Trible, R.P., and Samelson, L.E. (1998). LAT palmitoylation: its essential role in membrane microdomains targeting and tyrosine phosphorylation during T cell activation. Immunity *9*, 239–246.